New Phytologist

Research

The F-box protein SlSAP1 and SlSAP2 redundantly control leaf and fruit size by modulating the stability of SlKIX8 and SlKIX9 in tomato

Wenju Li[1,2]*, Mingli Liu[1,2]*, Renyin Wang[3], Liangliang He[1], Shaoli Zhou[1], Baolin Zhao[1], Yawen Mao[1], Qing Wu[1], Dongfa Wang[1], Xiaomin Ji[1,4], Jing Yang[1,5], Xiaoting Xie[1,4], Yu Liu[1], Shuang Wu[3], Jianghua Chen[1,4,5] and Liling Yang[1,3]

[1]State Key Laboratory of Plant Diversity and Specialty Crops, Xishuangbanna Tropical Botanical Garden, Chinese Academy of Sciences, Kunming, Yunnan, 650223, China; [2]School of Agriculture, Yunnan University, Kunming, 650504, China; [3]College of Horticulture, FAFU-UCR Joint Center and Fujian Provincial Key Laboratory of Haixia Applied Plant Systems Biology, Fujian Agriculture and Forestry University, Fuzhou, 350002, China; [4]University of Chinese Academy of Sciences, Beijing, 100049, China; [5]Yunnan Key Laboratory of Plant Reproductive Adaptation and Evolutionary Ecology and Institute of Biodiversity, School of Ecology and Environmental Science, Yunnan University, Kunming, Yunnan, 650500, China

Authors for correspondence:
Jianghua Chen
Email: jhchen@xtbg.ac.cn

Liling Yang
Email: yangliling@xtbg.ac.cn

Received: *11 December 2024*
Accepted: *21 March 2025*

New Phytologist (2025)
doi: 10.1111/nph.70159

Key words: fruit size, *SlKIX8*, *SlKIX9*, *SlSAP1*, *SlSAP2*, tomato, ubiquitination pathway.

Summary

- Tomato fruit size is a crucial trait in domestication, determined by cell division and cell expansion. Despite the identification of several quantitative trait loci associated with fruit size in tomatoes, the underlying molecular mechanisms that govern cell division and expansion to control fruit size remain unclear.
- CRISPR/Cas9 gene editing was used to generate single and double loss-of-function mutants of the tomato *STERILE APETALA1* (*c*) and *SlSAP2*. The results demonstrate that the two *SlSAP* genes function redundantly in regulating leaf and fruit size by positively regulating cell proliferation and expansion, with *SlSAP1* having the predominant effect. Consistently, overexpression of either *SlSAP1* or *SlSAP2* leads to enlarged fruits due to an increase in both cell layers and cell size in the pericarp.
- Biochemical evidence suggests that both SlSAP1 and SlSAP2 can form an SCF complex and physically interact with SlKIX8 and SlKIX9, which are crucial negative regulators of fruit size. Further results reveal that SlSAP1 and SlSAP2 target them for degradation.
- This study uncovers that the ubiquitination pathway plays an important role in the determination of tomato fruit size, and offers new genetic loci for improving fruit yield and biomass by manipulating pericarp thickness.

Introduction

Fruit size is an important indicator of crop yield and quality, as well as an adaptive feature in horticulture plants, which are becoming increasingly essential for human life (Mauxion *et al.*, 2021; Zhao *et al.*, 2021). The exploration of molecular pathways underlying fruit size has huge scientific and economic value (Wang *et al.*, 2024). The ultimate size of the fruit is determined by a complex process that involves the coordination of two interconnected cellular events: cell division and cell expansion (Mauxion *et al.*, 2021). Several key regulators have been revealed to independently or simultaneously regulate cell division and cell expansion, including hormonal signaling pathways, the CLV-WUS signaling pathway, the MADS-box gene family, the ubiquitin-proteasome pathway, quantitative trait loci (QTLs), microRNAs, and endoreduplication in model plants (Azzi *et al.*, 2015; Zhao *et al.*, 2021). Among these, the ubiquitin-proteasome pathway has received particular attention as it is one of the primary pathways for protein degradation and developmental regulation in plants (Li *et al.*, 2019; Varshney & Majee, 2022). The ubiquitination of proteins is carried out through the coordination of ubiquitin-activating enzyme (E1), ubiquitin-conjugating enzyme (E2), and ubiquitin ligase (E3). The SKP1/Cullin1/F-box (SCF) E3 ligase is a multi-subunit ligase composed of SKP1, Cullin1, RBX1, and an F-box protein (Varshney & Majee, 2022). Among these components, F-box proteins play an essential role in ensuring specificity in recognizing and targeting the substrates for degradation. Numerous studies have highlighted the crucial role of the F-box protein in regulating hormone signaling, stress responses, and organ development in the model plant Arabidopsis (Wang *et al.*, 2003; H. Huang *et al.*, 2023; Rieu *et al.*, 2023; Saxena *et al.*, 2023). The Arabidopsis F-box protein STERILE APETALA (SAP) functions as part of the SCF E3 ubiquitin ligase complex and significantly affects organ size by promoting

*These authors contributed equally to this work.

the proliferation of meristemoid cells (Wang *et al.*, 2016; Liu *et al.*, 2020). This is achieved through the targeted degradation of KINASE-INDUCIBLE DOMAIN INTERACTING 8/9 (KIX8/9)-PEAPOD1/2 (PPD1/2), which represses lateral organ growth by limiting the proliferation of meristemoid cells (Wang *et al.*, 2016; Li *et al.*, 2018). The SAP-KIX-PPD module has also been found to play an important role in determining organ size in other species. For instance, in *Capsella rubella*, decreased SAP activity results in shortened cell proliferation period and reduced number of petal cells (Sicard *et al.*, 2016); loss-of-function of *SMALL LEAF AND BUSHY1* (*SLB1*)/*MINI ORGAN1* (*MIO1*), a homolog of *SAP*; and decreased seed and leaf size in *Medicago truncatula* (Yin *et al.*, 2020; Zhou *et al.*, 2021; Mao *et al.*, 2023). Similar phenotypes have been reported in several other species that develop dry fruits, such as poplar (*Populus tremula*), cotton (*Gossypium hirsutum*), and Chinese cabbage (*Brassica rapa* L. ssp. *pekinensis*) (Liu *et al.*, 2019, 2022; Huang *et al.*, 2020; Azeez & Busov, 2021; Mauxion *et al.*, 2021). Additionally, loss-of-function of *LITTLELEAF* (*LL*), which is the homolog of *SAP* in the fleshy fruit species cucumber (*Cucumis sativus* L.), resulted in reduced size of leaves, flowers, fruits, and seeds, combined with increased lateral branches (Yang *et al.*, 2018). However, the detailed role of *SAP* homologs in other fleshy fruit species still remains to be elucidated.

Tomato (*Solanum lycopersicum* L.) is a typical fleshy fruit, and its fruit size is an important agricultural trait related to yield and quality (Mauxion *et al.*, 2021). The size of tomato fruits is primarily determined by the number of locules and pericarp thickness (Mauxion *et al.*, 2021). Increased floral meristem size has been shown to significantly enhance the number of locules, resulting in larger fruits (Xu *et al.*, 2015; Yuste-Lisbona *et al.*, 2020). This process is mainly determined by a conserved WUS-CLV feedback loop signaling pathway during the early stage of flower development (Zsögön *et al.*, 2018; Chu *et al.*, 2019; Kwon *et al.*, 2022; Aguirre *et al.*, 2023). Another factor contributing to fruit size is the thickness of the pericarp, which is the fleshy part of the fruit. The pericarp differentiates from the peripheral layer of the ovary and undergoes cell division and expansion during and after flower development (Mauxion *et al.*, 2021). The final thickness of the pericarp is determined by differential rates of cellular proliferation and expansion across different cell lineages and developmental stages. Approximately 30 QTLs related to fruit size or weight have been identified in tomato, and several of them exert significant roles in fruit size regulation, such as *fruit weight 1.1* (*fw1.1*), *fw2.2*, *fw3.1*, *fw3.2*, *fw4.1*, *fw9.1*, and *fw11.3* (Tanksley, 2004). So far, only three genes corresponding with these QTLs (*fw2.2*, *fw3.2*, and *fw11.3*) have been cloned in tomato, and the other functions remain to be fully elucidated (Azzi *et al.*, 2015). Both the *fw2.2* and *fw3.2* loci affect cell number and finally control tomato fruit biomass. Cytological analysis revealed that *fw2.2* decreases cell number, while *fw3.2* increases the number of pericarp cell layers (Frary *et al.*, 2000; Cong & Tanksley, 2006; Chakrabarti *et al.*, 2013; Monforte *et al.*, 2014; Tran & Billakurthi, 2024). The *fw11.3* QTL is associated with the *CELL SIZE REGULATOR* (*CSR*) gene, which increases the cell size of the mesocarp without altering the number of cell layers, resulting in the thicker pericarp and larger fruit (Mu *et al.*, 2017). However, the current understanding of fruit size determination in tomatoes is insufficient for molecular design breeding. Further functional studies on the regulation of fruit size are essential for tomato molecular breeding in order to identify valuable candidate genes and genetic loci.

In this study, we searched the whole genome sequence of tomato and identified two homologs of *AtSAP*, named *SlSAP1* and *SlSAP2*, respectively. Genetic analysis revealed that both *SlSAP1* and *SlSAP2* redundantly regulate fruit and leaf size. Molecular evidence suggests that both SlSAP1 and SlSAP2 are capable of forming the SCF complex and interacting with two important negative regulators of fruit size, SlKIX8 and SlKIX9. This implies that SlSAP1, SlSAP2, SlKIX8, and SlKIX9 function within the same pathway to regulate fruit size. Our results provide a genetic module for understanding the determination of fruit size and offer a new genetic tool for enhancing fruit yield and biomass in tomato.

Materials and Methods

Plant materials and growth conditions

All plants used in this study were of the tomato (*S. lycopersicum* L.) accessions Micro-Tom (MT) and Ailsa Craig (AC) background. We used MT as the wild-type (WT) to generate both overexpression and CRISPR/Cas9 transgenic plants of *SlSAP1* and *SlSAP2*, and AC as the WT to generate CRISPR/Cas9 transgenic plants of *SlSAP1* and *SlSAP2*. All WT and transgenic plants were cultured in glasshouses at the standard temperature and light conditions (16 h : 8 h, 24°C : 22°C, light : dark). The T2 generation plants were grown in the glasshouses, and all data were collected from them. Tobacco plants used for Split-LUC assays were also cultivated under the same glasshouse conditions. The plants were well-watered and supplied with adequate nutrients.

Phylogenetic analysis

Phylogenetic analysis was performed by retrieving *SlSAP1* and *SlSAP2* homologs from Phytozome 13 (https://phytozome-next.jgi.doe.gov/) for most species. Solanaceae homolog sequences were identified through a Blastp search from the Solanaceae Genomics Network (https://solgenomics.net/).

We identified all homologs with similar protein sequences to SlSAP1 and SlSAP2 from chlorophytes, mosses, ferns, gymnosperms, basal angiosperms, monocots, basal eudicots, and core eudicots (https://phytozome-next.jgi.doe.gov/). Phylogenetic trees were constructed using Mega 6 software. Sequences were aligned using ClustalW and then phylogenetic analyses were conducted using the Neighbor–Joining (NJ) method (Liu *et al.*, 2023). The amino acid sequences used in the construction of the phylogenetic tree are listed in Supporting Information Dataset S1.

Vector construction and tomato transformation

Gene sequence information was obtained from PHYTOZOME 13 (https://phytozome-next.jgi.doe.gov/). For the *cr-slsap1*, *cr-slsap2*, and *cr-slsap1/cr-slsap2* CRISPR knockout vectors, target sites were designed using the CRISPR-PLANT web tool (http://crispr.hzau.edu.cn/CRISPR2/) and inserted into the SlpTX041 vector. For the *35S:SlSAP1-eGFP* and *35S:SlSAP2-eGFP* vectors, the coding sequences (CDSs) of *SlSAP1* and *SlSAP2* were inserted between the CaMV 35S promoter and eGFP using the ClonExpress II One Step Cloning Kit (C112-01; Vazyme Biotech, Nanjing, China). The constructed vectors were transformed into *Agrobacterium tumefaciens* EHA105 for stable tomato transformation. Genomic DNA from the transgenic plants was extracted using the CTAB method and used for the verification of the CRISPR knockout lines. Primer information is shown in Table S1.

Quantitative real-time reverse-transcriptase PCR (qRT-PCR) analysis

To analyze the expression patterns of *SlSAP1* and *SlSAP2*, 5-wk-old tomato plants grown under similar conditions were used for tissue collection, including roots, hypocotyls, cotyledons, stems, leaves, flowers, sepals, petals, stamens, carpels, and flowers at different developmental stages (Yang *et al.*, 2020). For analyzing the expression levels of the target genes in *OE-SlSAP1* and *OE-SlSAP2* transgenic plants, young leaves from 3-wk-old T1 generation plants and WT were collected for analysis. Total RNA was extracted from different tissues using the RnaEx™ Total RNA Isolation Solution (GK3006; GENEray, Shanghai, China) according to the manufacturer's instructions. First-strand cDNA was synthesized from 1 μg of total RNA using the HIScript II 1st Strand cDNA Synthesis Kit (R212-02; Vazyme Biotech). Quantitative real-time PCR was performed with a LightCycler 480II Real-Time System (Roche) using the QuantFast SYBR Green qPCR Super Mix (M2211; Magic-Bio, Hangzhou, China). The PCR reaction conditions were as follows: 94°C for 3 min, followed by 40 cycles of 94°C for 5 s and 60°C for 30 s. The specificity of PCR amplification was verified by a dissociation curve analysis (65–95°C). Relative gene expression was calculated using the $2^{-\Delta\Delta C_t}$ method. *SlACTIN2* was used as the reference gene to normalize gene expression. All analyses were performed with three biological replicates and three technical replicates. The primers used are listed in Table S1.

Subcellular localization analysis

The constructs *35S:SlSAP1-eGFP*, *35S:SlSAP2-eGFP*, and the corresponding empty vector pHellsgate 8 (*35S:eGFP*) were transformed into *A. tumefaciens* strain EHA105 and infiltrated into the leaves of 5-wk-old *Nicotiana benthamiana* for transient expression. The infiltrated plants were incubated in the dark at 22°C for 24 h and then exposed to 16 h of light at 24°C, followed by 8 h of darkness at 22°C for 1 d before observing GFP signals using confocal microscopy (LSM 880; Carl Zeiss). The primers are listed in Table S1.

Histological analysis

Histological analysis was performed as previously described. Briefly, the fruits from WT, *cr-slsap1*, *cr-slsap2*, *cr-slsap1/2*, *OE-SlSAP1*, and *OE-SlSAP2* transgenic plants at different developmental stages (0, 3, 5, 8, 15, and 30 d) were fixed overnight at 4°C in FAA solution. The samples were then dehydrated through a graded series of ethanol and xylene, followed by embedding in a paraffin solution containing 50% xylene for 4 h. After infiltration, the samples were placed in pure paraffin (Sigma-Aldrich) overnight.

Sections (10 μm thick) were cut using a Leica RM225587 microtome (Leica, Wetzlar, Germany), and the paraffin was removed by treatment with xylene for 30 min. The tissue sections were then carefully washed in distilled water and stained for 1 min with 0.25% toluidine blue-O (Sigma-Aldrich). All micrographs were captured using an Olympus BX63 light microscope (Olympus Corp., Tokyo, Japan). The cell layer number and individual cell area were quantified using IMAGEJ (https://imagej.nih.gov/ij/). For each genotype, 10–20 biological replicates were analyzed.

Yeast two-hybrid (Y2H) assay

The Matchmaker GAL4 Two-Hybrid System was utilized in this study to screen a cDNA library and analyze protein–protein interactions. To identify proteins that interact with SlSAP1, we constructed a yeast cDNA library using the shoot apical tissues of Ailsa Craig. The CDS of *SlSAP1* was cloned into the pGBKT7 vector as a bait vector (BD-SlSAP1). Before screening the library, we assessed the autonomous activation of BD-SlSAP1 by culturing the yeast strain Y2H Gold containing BD-SlSAP1 and the empty pGADT7 vector on SD/−Trp/−Leu/−His/−Ade (QDO) agar medium. Subsequently, Y2H Gold strains containing BD-SlSAP1 were mixed with the Y187 strains harboring the library proteins for mating. The mated cells were spread on QDO medium at 30°C for 4–6 d to screen for positive colonies. Each clone was selected individually for PCR and then used to identify the corresponding interacting proteins in the *S. lycopersicum* genome.

For protein–protein interaction analysis, the CDSs of *SlSAP1* and *SlSAP2* were constructed into the pGBKT7 vector (bait vector), while *SlASK1*, *SlASK2*, *SlASK3*, *SlKIX8*, and *SlKIX9* were constructed into the pGADT7 vector (prey vector). Pairs of recombinant constructs were co-transformed into the yeast strain Y2H Gold and cultured on SD/−Trp/−Leu (DDO) medium for 3–4 d. The co-transformed yeast cells were suspended in sterile ddH_2O to an OD_{600} of 1 and then cultured on QDO medium for 3 d. For each combination, three replicates were conducted, and one of the replicates is presented in the figure. All of the used primers are listed in Table S1.

Luciferase (LUC) assay

The CDSs of *SlSAP1* and *SlSAP2* were constructed into the pCAMBIA1300-nLUC vector, while the CDSs of *SlASK1*, *SlASK2*, *SlASK3*, *SlKIX8*, and *SlKIX9* were constructed into the

pCAMBIA1300-cLUC vector. The constructed vectors were transformed into the *A. tumefaciens* strain EHA105. Equal volumes of *Agrobacterium* harboring different constructs were mixed and co-infiltrated into the leaves of 5-wk-old *N. benthamiana* for transient expression (Wang *et al.*, 2016). LUC activity was determined using the Dual-Luciferase® reporter analysis system (Promega) kit, and the infiltrated areas were examined for luciferase activity using a cooled low-light CCD camera (5200; Tanon, Shanghai, China) after 3 d. All of the used primers are listed in Table S1.

Degradation assay

To express fusion proteins for the degradation assay, the CDSs of *SlKIX8* and *SlKIX9* were cloned into the pMAL-c5X vector using the homologous recombination system to generate MBP-SlKIX8 and MBP-SlKIX9 fusion proteins, respectively. The MBP-SlKIX8 and MBP-SlKIX9 fusion proteins were expressed in *Escherichia coli* strain Transetta (DE3), induced with 250 μM isopropyl-β-D-thiogalactoside (IPTG) at 28°C, and purified using amylose resin (E8021S; New England Biolabs, Ipswich, MA, USA) according to the manufacturer's instructions. Total protein was extracted from an equal amount of flower tissue using protein extraction buffer (50 mM HEPES (pH 7.5), 50 mM NaCl, 10 mM EDTA, 0.2% Triton X-100, 10% Glycerol, 2 mM DTT, 100 μM PMSF, 1× Cocktail, 10 mM ATP) from the WT, *cr-slsap1/cr-slsap2* double mutants, and *SlSAP1* and *SlSAP2* overexpression lines. Then, the purified MBP-SlKIX8 and MBP-SlKIX9 fusion proteins were mixed with the total protein solution, respectively, at a 1 : 3 volume ratio. For the control, the total protein was pretreated with 50 μM MG132 before being mixed with MBP-SlKIX8 and MBP-SlKIX9. All the mixtures were incubated at 4°C with gentle shaking. Samples were collected at different time points (0 and 45 min), and the catalytic reaction was stopped by boiling for 10 min at 98°C in SDS loading buffer. The denatured protein was separated on a 10% SDS-PAGE gel and detected by immunoblot analysis using anti-MBP antibodies (HT701-01; Transgene, Beijing, China). Equal amounts of the total proteins were used as loading controls (Liu *et al.*, 2010). The method described above was used with some modifications to compare the protein degradation efficiency between SlSAP1 and SlSAP2. Total protein was extracted from an equal amount of flower tissue using a protein extraction buffer from the WT, *cr-slsap1*, *cr-slsap2*, and *cr-slasp1 cr-sap2* mutants. The incubation times were 0, 45, and 90 min.

Analysis of leaf growth parameter

The fourth and fifth leaves (counted from bottom to top) of 60-d-old CRISPR-Cas mutants, overexpressed transgenic lines, and WT plants were harvested to analyze leaf growth parameters. For each genotype, 30 biological replicates (leaves) were collected. The biomass/fresh weight of the whole leaf and its terminal leaflets were measured using a digital balance (Yin *et al.*, 2023). The leaves were then cut and flattened for photographing the actual leaflet area (Swinnen *et al.*, 2022). The true leaflet area was quantified using ImageJ software (https://imagej.nih.gov/ij/).

Analysis of ovary growth parameter

To measure the diameter, height, and weight of the ovary, fruits from CRISPR-Cas mutants, overexpressed transgenic lines, and WT plants were harvested at different time points before pollination. The diameter of the ovary was quantified by averaging the maximum and minimum diameters along the equatorial axis. For each genotype, 30 biological replicates (ovaries) were collected and analyzed.

Analysis of fruit growth parameter

To measure fruit weight and peel thickness, fruits at different developmental and ripening stages (from 0 d post-anthesis (DPA) to red ripening) were harvested from CRISPR-Cas mutants, overexpressed transgenic lines, and WT plants. Fruit diameter and height were measured using ImageJ. The error bars represent the SD of the mean for all values. Statistical analyses were performed using GraphPad Prism (v.9.0.5).

Results

Identification of the *SAP* homologs in Solanaceae

The fruit size of tomato is an important agronomic trait that determines both yield and quality (Mauxion *et al.*, 2021). The molecular mechanisms behind the fruit size determination remain a key question to be answered in the future. Previous studies have indicated that the *SAP* gene and its homologs act as positive regulators of leaf and seed size in some plants that produce dry fruits (Wang *et al.*, 2016; Yordanov *et al.*, 2017; Yin *et al.*, 2020; Liu *et al.*, 2022). However, it is still unknown whether the *SAP* homologs play an important role in the determination of fresh fruit size in tomato. In this study, we identified two putative *SAP* genes in the tomato genome, *SlSAP1* and *SlSAP2*, which are highly homologous to the previously reported *SAP* gene in *Arabidopsis thaliana* (Fig. 1a). Unlike the single *SAP* ortholog reported in Arabidopsis, Medicago, cucumber, Chinese cabbage, and poplar, tomato harbors two *SAP* homologs (Fig. 1a, b). We constructed a phylogenetic tree of SAP proteins from a broad range of species representing major plant lineages, including six species within the Solanaceae family, as well as several species with previously reported SAP members, and some basal plant species. The results revealed that SAP proteins first appeared in ferns and are universally present in gymnosperms and eudicots; they are also found in some monocots but absent in Poaceae, algae, and mosses (Fig. 1a,b). Furthermore, we found that two *SAP* homologs are commonly observed in Solanaceae plants, and tetraploid tobacco even contains four *SAP* homologs (Fig. 1a,b).

Sequence analysis revealed that SlSAP1 and SlSAP2 exhibit comparable molecular lengths, with SlSAP1 comprising 450 amino acids and SlSAP2 consisting of 437 amino acids. Then NCBI Blast alignment of the two sequences demonstrated a high degree of sequence similarity, with a calculated identity of 67%, indicating a substantial conservation (Fig. S1). 3D

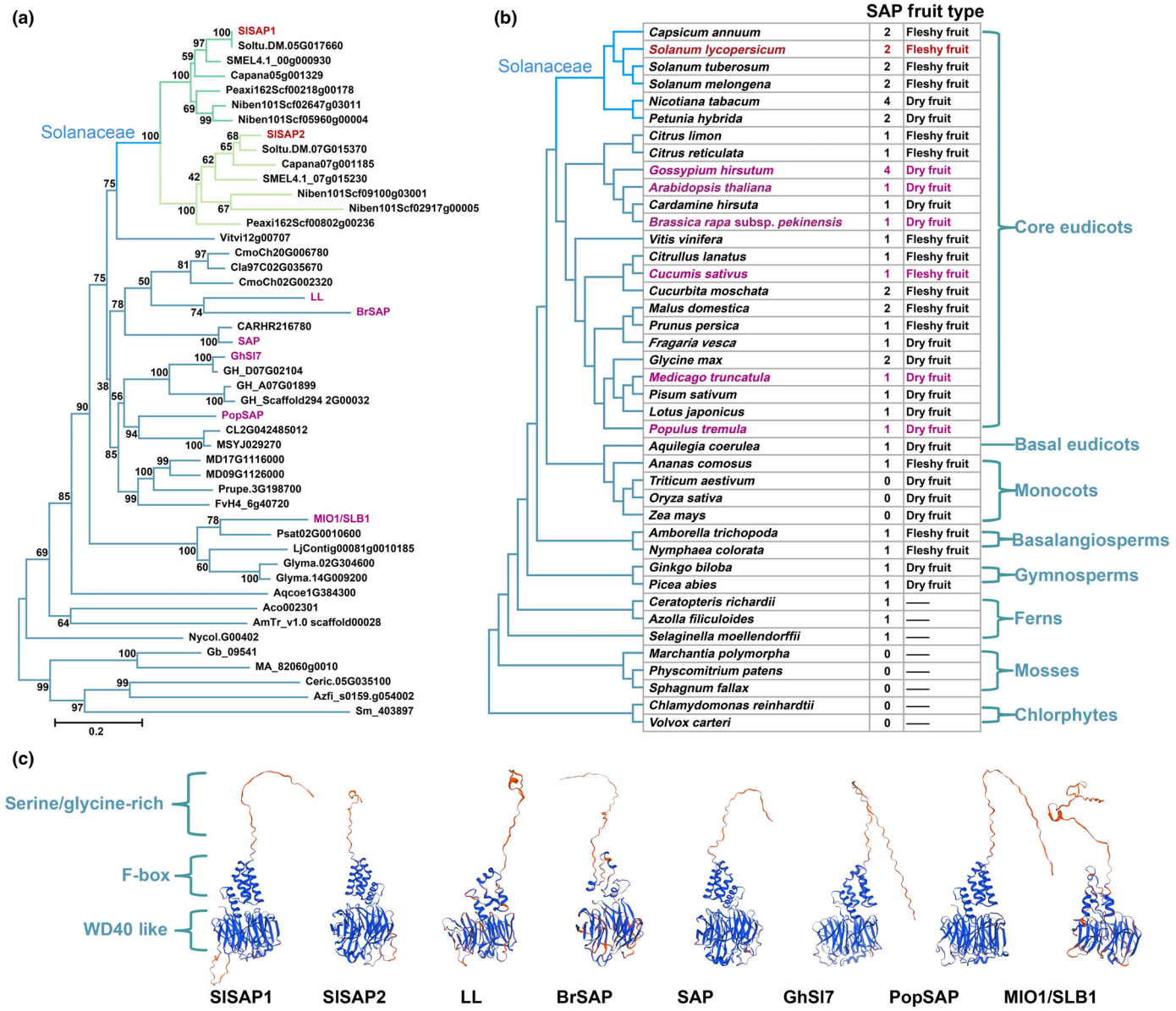

Fig. 1 Phylogenetic analysis supports the presence of two *STERILE APETALA* (*SAP*) homologs in the Solanaceae family. (a) Phylogeny of *STERILE APETALA1* (SlSAP1) and *STERILE APETALA2* (SlSAP2) and their homologs from various species is presented. Bootstrap values at the nodes of the tree are percentages from 1000 replicates. Branch length indicates the number of substitutions per site. The red font and the pink font indicate SlSAP1 and SlSAP2 identified in this work and their homologs with functional reports, respectively. The two classes of SAP homologs in the Solanaceae family are indicated by a dark green line and a light green line, respectively. (b) The number of SlSAP1 and SlSAP2 homologs identified in each species is shown. The table on the right summarizes the types of fruit (dry fruits or fleshy fruits). (c) Protein structures predicted by SWISS-MODEL for SlSAP1, SlSAP2, LL, BrSAP, SAP, GhSI7, PopSAP, and *MINI ORGAN1/SMALL LEAF AND BUSHY1* (MIO1/SLB1) are presented. All homologs of SlSAP1 and SlSAP2 share the conserved Ser/Gly-rich domain, the F-box domain, and the WD40-like domain.

structure prediction analysis further showed that SlSAP1 and SlSAP2 contain the same domains: a serine/glycine-rich domain and an F-box motif at the amino terminus, as well as a WD40-like domain in the carboxy-terminal region (Fig. 1c). All of the domains are conserved among the previously reported homologs in Arabidopsis (SAP), Medicago (SLB1/MIO1), cucumber (LL), Chinese cabbage (BrSAP), cotton (GhSI7), and poplar (PopSAP) (Fig. 1c). These results indicate that both SlSAP1 and SlSAP2 are classic F-box proteins that are highly conserved in most eudicots.

Expression pattern analysis of *SlSAP1* and *SlSAP2* and the subcellular localization of their encoded proteins

We performed the quantitative real-time reverse-transcriptase PCR (qRT–PCR) analysis to investigate the expression pattern of *SlSAP1* and *SlSAP2*. The results revealed that both *SlSAP1* and *SlSAP2* are prominently expressed in flower and root, with *SlSAP1* exhibiting a higher level of expression than *SlSAP2* (Fig. 2a). Given their high expression in flower, we further tested the expression patterns of *SlSAP1* and *SlSAP2* in different floral

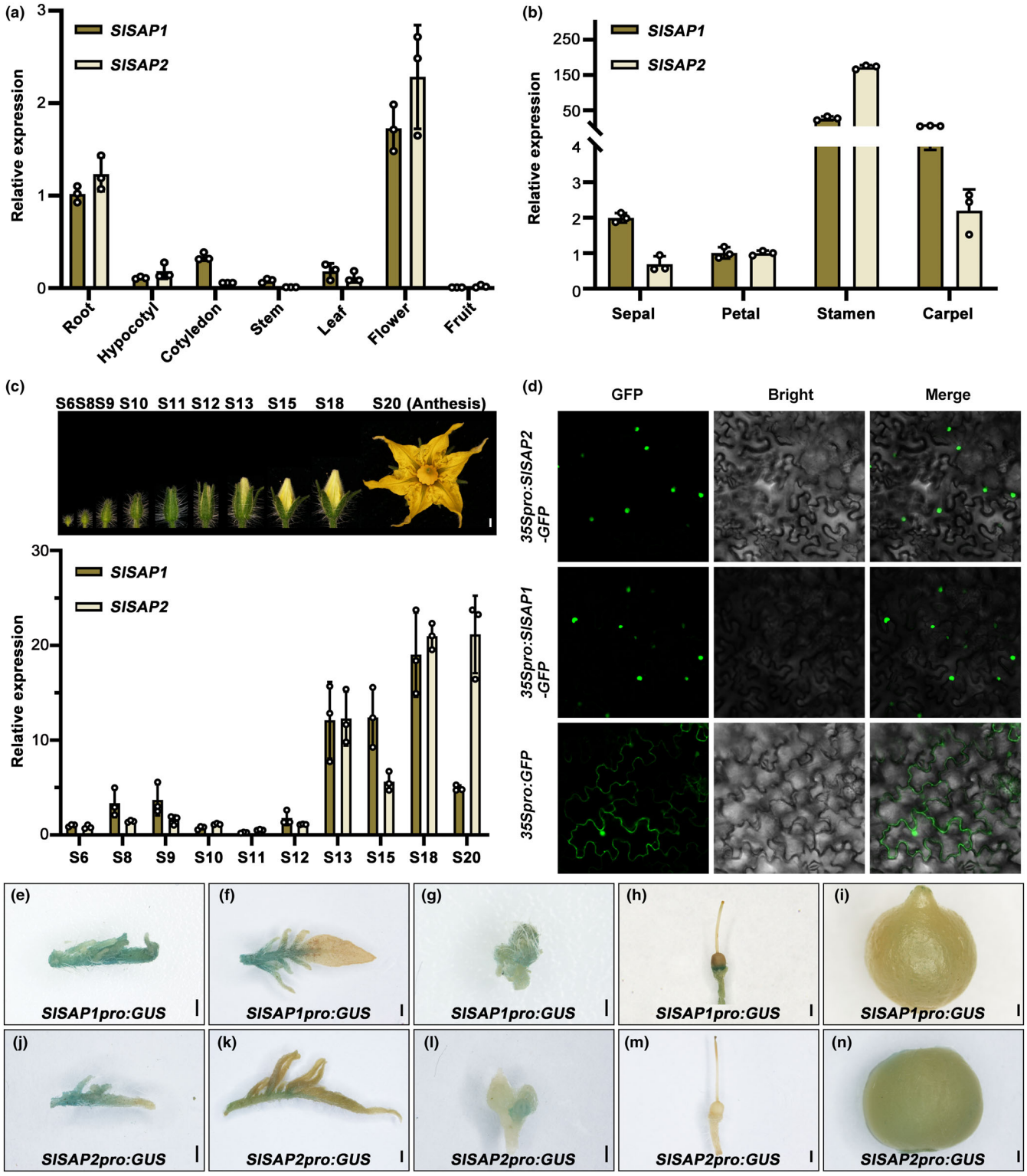

Fig. 2 Expression patterns of *STERILE APETALA1* (*SlSAP1*) and *STERILE APETALA2* (*SlSAP2*) and subcellular localization of the encoded proteins. (a–c) Quantitative real-time reverse-transcriptase PCR (qRT-PCR) analysis of the relative expression levels of *SlSAP1* and *SlSAP2* in different tissues (a), various floral organs (b), and at different developmental stages of flowers (c) in the tomato Micro-TOM ecotype. *SlACTIN2* was used as the internal control in (a–c). Error bars represent the SD from three biological replicates. (d) Subcellular localization of eGFP, SlSAP1–eGFP, and SlSAP2–eGFP in tobacco epidermal cells. GFP, green fluorescent protein. (e–i) β-Glucuronidase (GUS) staining of young leaves (e, f), inflorescences (g), carpels (h), and 10 d post-anthesis (DPA) fruits (i) from *SlSAP1pro:GUS* transgenic plants in the tomato Ailsa Craig ecotype. (j–n) GUS staining of young leaves (j, k), inflorescences (l), carpels (m), and 10 DPA fruits (n) from *SlSAP2pro:GUS* transgenic plants in the tomato Ailsa Craig ecotype. S, stage; S6, 6th stage of flower development; S20, 20th stage of flower development. Bars: (e–n) 1 mm.

organs. The results showed that *SlSAP1* and *SlSAP2* are highly expressed in stamens and carpels (Fig. 2b), indicating that they may play important roles in stamen and carpel development. Therefore, we further analyzed their temporal expression patterns during floral development. The results showed that the expression of *SlSAP1* and *SlSAP2* exhibited temporal specificity, with elevated transcript abundance observed from stages 15–20 of floral development (Fig. 2c). In addition, we tested the expression patterns of *SlSAP1* and *SlSAP2* at different fruit developmental stages. The results showed that *SlSAP1* and *SlSAP2* are expressed at 15 and 30 DPA (Fig. S2). To further confirm this, we introduced the GUS reporter gene driven by the *SlSAP1* and *SlSAP2* promoters into the WT (AC ecotype), respectively. GUS signals were detected in young leaves, inflorescences, stamens, and 10 DPA fruits in both *SlSAP1pro:GUS* and *SlSAP2pro:GUS* transgenic lines (Fig. 2e–n). Additionally, GUS signals were detected in the proximal region of the carpel in *SlSAP1pro:GUS* plants but not in *SlSAP2pro:GUS* plants (Fig. 2h,m).

To determine the subcellular localization of SlSAP1 and SlSAP2, we transiently expressed SlSAP1-green fluorescent protein (GFP) and SlSAP2-GFP fusion proteins under the control of the cauliflower mosaic virus 35S promoter in tobacco leaf cells. Confocal microscopy revealed nuclear-specific GFP fluorescence for both 35S:SlSAP1-eGFP and 35S:SlSAP2-eGFP (Fig. 2d), indicating the nuclear localization of both proteins.

SlSAP1 and *SlSAP2* redundantly regulate tomato leaf and fruit size, with *SlSAP1* playing a dominant role

To elucidate the biological functions of *SlSAP1* and *SlSAP2* in tomato, CRISPR/Cas9 was used to knock out *SlSAP1* and *SlSAP2* in the Micro-Tom cultivar. We selected the target sites from 273 to 292 bp downstream of the translation initiation site (TIS) of *SlSAP1* and from 434 to 452 bp downstream of the TIS of *SlSAP2* (Fig. 3a,b). A slight dwarf plant architecture was observed in *cr-slsap1* mutants (Figs 3c,d, S3c). Furthermore, mature leaf size, flower size, and fruit size were smaller than those of WT (Figs 3g,h,k,l, S3i,f,l). *cr-slsap2* mutants also showed slight reductions in plant height, leaf size, flower size, and fruit size, but the phenotype was weaker than that of *cr-slsap1* mutants (Figs 3c,g,k,e,i,m, S3d,j,g,m). Statistical analysis of the leaf fresh weights of *cr-slsap1* and *cr-slsap2* leaves showed a decrease of 78.3% and 39.9%, respectively, when compared with WT leaves (Fig. 3o). The leaf areas of *cr-slsap1* and *cr-slsap2* leaves were 69.8% and 35.7% smaller, respectively, than those of the corresponding WT leaves (Fig. 3p). The height and diameter of individual ripe tomato fruits from *cr-slsap1* plants were reduced by 27.6% and 34.1%, respectively, compared to those from WT plants (Fig. 3q,r). Similarly, the height and diameter of individual ripe fruits from *cr-slsap2* plants decreased by 19.8% and 15.8%, respectively, compared to WT plants (Fig. 3q,r). In line with this, the fresh weight of individual ripe tomatoes produced by *cr-slsap1* and *cr-slsap2* plants was reduced by 62.2% and 35%, respectively, compared with those of WT (Fig. 3s). These findings, in conjunction with the higher expression level of *SlSAP1* compared to *SlSAP2* in different organs (Fig. 2a), suggest that both *SlSAP1* and *SlSAP2* play crucial roles in regulating organ size, with *SlSAP1* having a predominant effect.

To further elucidate the functions of *SlSAP1* and *SlSAP2* in tomato organ development regulation, we examined the phenotype of the *cr-slsap1 cr-slsap2* double mutants. An extreme reduction in plant height, leaf size, and flower size was observed in three independent knock-out lines, *cr-slsap1 cr-slsap2-L5*, *cr-slsap1 cr-slsap2-L6*, and *cr-slsap1 cr-slsap2-L9* (Figs 3c,g,k,f,g,n, S3e,k,h,n). The leaf fresh weights of the double mutants were 90.5% smaller than those of corresponding WT, leaves (Fig. 3o), and the leaf area in *cr-slsap1 cr-slsap2* double mutants was 83.5% lower than that of WT leaves (Fig. 3p). Additionally, compared to WT, the height and diameter of individual ripe tomato fruits of the *cr-slsap1 cr-slsap2* double mutants were decreased by 44.1% and 39.4%, respectively (Fig. 3q,r), and the fresh weight of individual ripe tomato fruit of these double mutants was reduced by 83.5% (Fig. 3s). Furthermore, compared to that of WT or either *cr-slsap1* or *cr-slsap2* single mutants, the number of leaflets per leaf was reduced in the *cr-slsap1 cr-slsap2* double mutants, which possessed only a pair of lateral leaflets and one terminal leaflet (Figs 3j, S3k). These results suggest that *SlSAP1* and *SlSAP2* play redundant roles in regulating tomato organ size and leaflet number, with the most substantial impact observed in fruit biomass, highlighting their critical influence on tomato fruit development. Similar results have been verified in the tomato AC ecotype background (Fig. S4a–p).

Overexpression of *SlSAP1* and *SlSAP2* leads to larger fruit size

To gain further insight into the function of *SlSAP1* and *SlSAP2*, we expressed the CDSs of *SlSAP1* and *SlSAP2* under the control of the *35S* promoter in WT plants, respectively. Expression of either *35S:SlSAP1-eGFP* or *35S:SlSAP2-eGFP* in the WT resulted in a range of modifications in both leaf and fruit development (Fig. 4a–i). A rippled, dome-shaped leaf phenotype was already observable in regenerated *35S:SlSAP1-eGFP* or *35S:SlSAP2-eGFP* tomato T0 plants. Similarly, the T1 plants expressing either *35S:SlSAP1-eGFP* (*35S:SlSAP1-eGFP-L8* and *35S:SlSAP1-eGFP-L13*) or *35S:SlSAP2-eGFP* (*35S:SlSAP2-eGFP-L11*, and *35S:SlSAP2-eGFP-L17*) displayed dome-shaped leaves with uneven leaf laminae (Fig. 4d–f). Consistently, the expression levels of *SlSAP1* and *SlSAP2* are significantly upregulated in the transgenic lines (Fig. 4j,k). Quantification of leaf areas and biomasses revealed only a slight increase in both parameters in the *35S:SlSAP1-eGFP* transgenic lines, with a more noticeable increase occurring in the terminal leaf (Fig. 4l–o).

However, overexpression of either *SlSAP1* or *SlSAP2* led to significantly larger fruits (Fig. 4g–i). To quantitatively assess these improvements, we measured the height, diameter, and biomass of the fruits in *SlSAP1* and *SlSAP2* overexpressed transgenic plants. Compared to WT plants, the average fruit height and diameter of *35S:SlSAP1-eGFP* transgenic plants increased by 0.28- and 0.17-fold compared to WT (Fig. 4p,q), while in *35S:SlSAP2-eGFP* transgenic plants, the fruit height and diameter increased by 0.26- and 0.14-fold (Fig. 4p,q). The average fresh

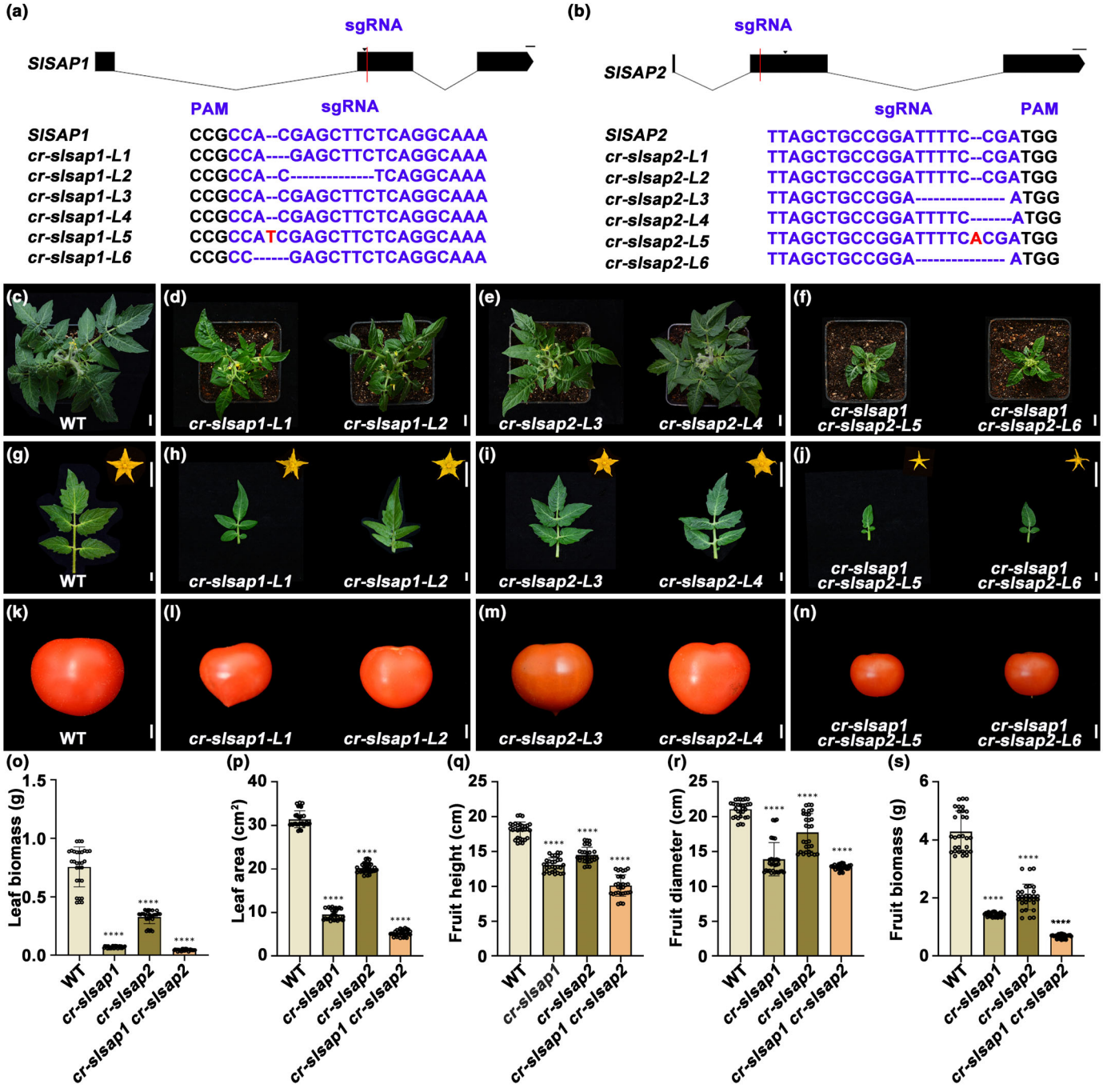

Fig. 3 CRISPR-Cas9 genome editing of tomato *STERILE APETALA1* (*SlSAP1*) and *STERILE APETALA12* (*SlSAP2*) results in the smaller leaf and fruit size phenotype. (a) Diagram of the *SlSAP1* gene and sequences of the different *SlSAP1* CRISPR alleles. The red line indicates the locations of the mutations, and the red letters indicate different mutations. (b) Diagram of the *SlSAP2* gene and sequences of the different *SlSAP2* CRISPR alleles. The red line indicates the locations of the mutations, and the red letters indicate different mutations. (c–f) The plants of the indicated genotypes were grown in soil for 1 month under glasshouse conditions, as described in the Materials and Methods section, and photographed from the top. (g–j) Mature 5th leaves (count from the bottom) and the fully opened flowers (at the top right corner of each picture) of the indicated genotypes. LL, lateral leaflet; TL, terminal leaflet. (k–n) Red-ripening fruits of the indicated genotypes. (o, p) Quantification of the biomass (o) and area (p) of the 5th leaves (count from the bottom) in the indicated genotypes. Error bars denote SE ($n = 30$). (q–s) Quantification of the height (q), diameter (r), and biomass (s) of red-ripening fruits in the indicated genotypes. Error bars denote SE ($n = 30$). *t*-test: ****, $P < 0.0001$. Bars: (c–n) 1 cm.

weights of *35S:SlSAP1-eGFP* and *35S:SlSAP2-eGFP* transgenic plants showed a 0.43- and 0.30-fold increase in total biomass, respectively (Fig. 4r). These results suggest that the overexpression of *SlSAP1* and *SlSAP2* results in only a modest increase in leaf size, but a significant increase in fruit size in tomato.

To further verify the role of *SlSAP1* and *SlSAP2* in regulating fruit size and to determine the influence of an altered sink–source relationship between *cr-slsap1 cr-slsap2* double mutants and WT plants, a follow-up experiment was performed in which fruit production was restricted. Specifically, only the first two inflorescences on the main shoot, each carrying a maximum of three fruits, were retained per plant, and fruit size was measured at the red-ripe stage. Although the fruit size of both WT and *cr-slsap1 cr-slsap2* double mutants was larger than that of plants without restricted fruit numbers (Fig. S5a–d), the fruit size of the *cr-slsap1 cr-slsap2* double mutants was smaller than that of WT plants (Fig. S5b,d). These results further suggest that *SlSAP1* and *SlSAP2* play a role in regulating fruit size.

Both *SlSAP1* and *SlSAP2* positively regulate fruit size by enhancing cell proliferation and cell expansion in the pericarp

To elucidate the underlying mechanisms of the different fruit sizes in the loss-of-function and gain-of-function *SlSAP1* and *SlSAP2* genetically modified lines, it is important to consider whether pericarp thickness or locule number contributes to final fruit size. First, the locule numbers in WT, *cr-slsap1*, *cr-slsap2*, *cr-slsap1 cr-slsap2*, *35S:SlSAP1-eGFP*, and *35S:SlSAP2-eGFP* transgenic lines were investigated, and the results showed no significant differences, with locule numbers ranging from two to four (Fig. 5a–f). Next, we compared the pericarp thickness of red-ripe fruit from these genetically modified lines. The results confirmed a decrease in pericarp thickness in the *cr-slsap1*, *cr-slsap2*, and *cr-slsap1 cr-slsap2* fruits, with the pericarps of these mutants being 24.7%, 21.5%, and 53% thinner, respectively, than those of WT (Fig. 5a–d,m,n). By contrast, the pericarp thickness of the *35S:SlSAP1-eGFP* and *35S:SlSAP2-eGFP* lines was increased by 83.4% and 67.2%, respectively, compared to WT (Fig. 5a,e,f,m,n). So we can conclude that the smaller fruit size in the loss-of-function *SlSAP1* and *SlSAP2* lines is due to decreased pericarp thickness, while the larger fruit size in the gain-of-function *SlSAP1* and *SlSAP2* transgenic lines is due to increased pericarp thickness. These indicate that *SlSAP1* and *SlSAP2* redundantly promote pericarp thickness, thereby influencing fruit size.

To explore the cellular basis of these changes in pericarp thickness in these genetically modified lines, we quantified the number of cell layers and cell sizes of the pericarp. At 30 DPA, the number of cell layers across the pericarp was found to be decreased in *cr-slsap1 cr-slsap2* fruits, but increased in *35S:SlSAP1-eGFP* and *35S:SlSAP2-eGFP* transgenic fruits (Fig. 5g–l,o). The average pericarp cell area was also decreased in *cr-slsap1*, *cr-slsap2*, and *cr-slsap1 cr-slsap2* mutant fruits compared to WT (Fig. 5g–j,p), whereas it was larger in *35S:SlSAP1-eGFP* and *35S:SlSAP2-eGFP* transgenic fruits (Fig. 5g,k,l,p). Further analysis revealed that the increased mean cell area in the *35S:SlSAP1-eGFP* and *35S:SlSAP2-eGFP* lines was due to a higher proportion of very large cells within the pericarp, while in the loss-of-function *SlSAP1* and *SlSAP2* lines, a higher proportion of small cells and a decreased proportion of very large cells were observed compared to WT plants (Fig. 5g–l,q). Altogether, these results demonstrate that *SlSAP1* and *SlSAP2* regulate pericarp thickness by positively regulating both cell proliferation and expansion.

SlSAP1 and SlSAP2 function within an SCF complex

SAP has been reported as a post-transcriptional regulator (White, 2006; Wang *et al.*, 2016). To understand the molecular mechanisms underlying the function of SlSAP1 and SlSAP2, we performed a Y2H screen to identify SlSAP1 interactors using a yeast cDNA library constructed from tomato shoot apical tissues. Three SKP1-like proteins (Solyc11g042930, Solyc01g111650, and Solyc10g055580) were highly enriched among the screened clones (Fig. S6a). Since the homologs of these proteins in Arabidopsis are ASK1 and ASK2, which are known as substrate-recruiting subunits of SKP1/Cullin/F-box-protein (SCF) complexes, we designated them SlASK1, SlASK2, and SlASK3, respectively (Fig. S6a,b). The Y2H assays validated the interactions between SlSAP1 and SlASK1/2/3, as well as between SlSAP2 and SlASK1/2/3 (Figs 6a, S6c).

To further verify whether SlSAP1 and SlSAP2 are able to form the SCF complex *in planta*, we performed split-luciferase assays to detect the interactions between SlSAP1 and SlASK1/2/3, as well as between SlSAP2 and SlASK1/2/3 *in vivo*. SlSAP1 and SlSAP2 were fused with the N-terminal fragment of luciferase (nLUC), while SlASK1/2/3 were fused with the C-terminal fragment of luciferase (cLUC), respectively. When these proteins were co-expressed in tobacco leaves, a specific luciferase activity signal was observed in the combination of SlSAP1 and SlASK1/2/3 (Fig. 6b–d). Similar results were also observed in the combination of SlSAP2 and SlASK1/2/3 (Fig. 6e–g), but no signal was detected in the control combinations (Fig. 6b–g). These results indicate that both SlSAP1 and SlSAP2 can interact with SlASK1/2/3 to form an SCF complex *in planta*.

SlSAP1/2 mediated degradation of SlKIX8/9 through physical interaction

Previous studies have shown that SAP regulates organ size by modulating the protein stability of PPD and KIX (Wang *et al.*, 2016; Li *et al.*, 2018; Yin *et al.*, 2020). Therefore, we investigated whether SlSAP1 and SlSAP2 physically interact with SlKIX8, SlKIX9, SlPPD1, and SlPPD2. The Y2H assays validated the interaction between SlSAP1/2 and SlKIX8, as well as between SlSAP1/2 and SlKIX9 in yeast cells (Fig. 7a). However, neither SlSAP1 nor SlSAP2 physically interacts with SlPPD1 or SlPPD2 (Fig. S7). We further performed split-luciferase assays to verify whether SlSAP1/2 physically associates with SlKIX8/9 *in planta*. SlSAP1 and SlSAP2 were each fused with nLUC, while SlKIX8 and SlKIX9 were each fused with cLUC. When these proteins were co-expressed in tobacco leaves, we observed a specific luciferase activity signal in the combinations of SlSAP1/2 with SlKIX8 (Fig. 7b,d), as well as SlSAP1/2 with SlKIX9 (Fig. 7c,e), and no signal in the control combinations (Fig. 7b–e).

Given the similar phenotypes observed in either *SlSAP1* or *SlSAP2* overexpression and the *cr-slkix8 cr-slkix9* double mutant

plants (Swinnen *et al.*, 2022), we investigated whether SlSAP1 and SlSAP2 could regulate the stability of SlKIX8 and SlKIX9 proteins in a proteasome-dependent manner since both SlSAP1 and SlSAP2 are capable of forming the SCF complex (Fig. 6a–g). To test this, total proteins were extracted from WT plants, *cr-slsap1 cr-slsap2* double mutants, and *SlSAP1*-overexpressed and

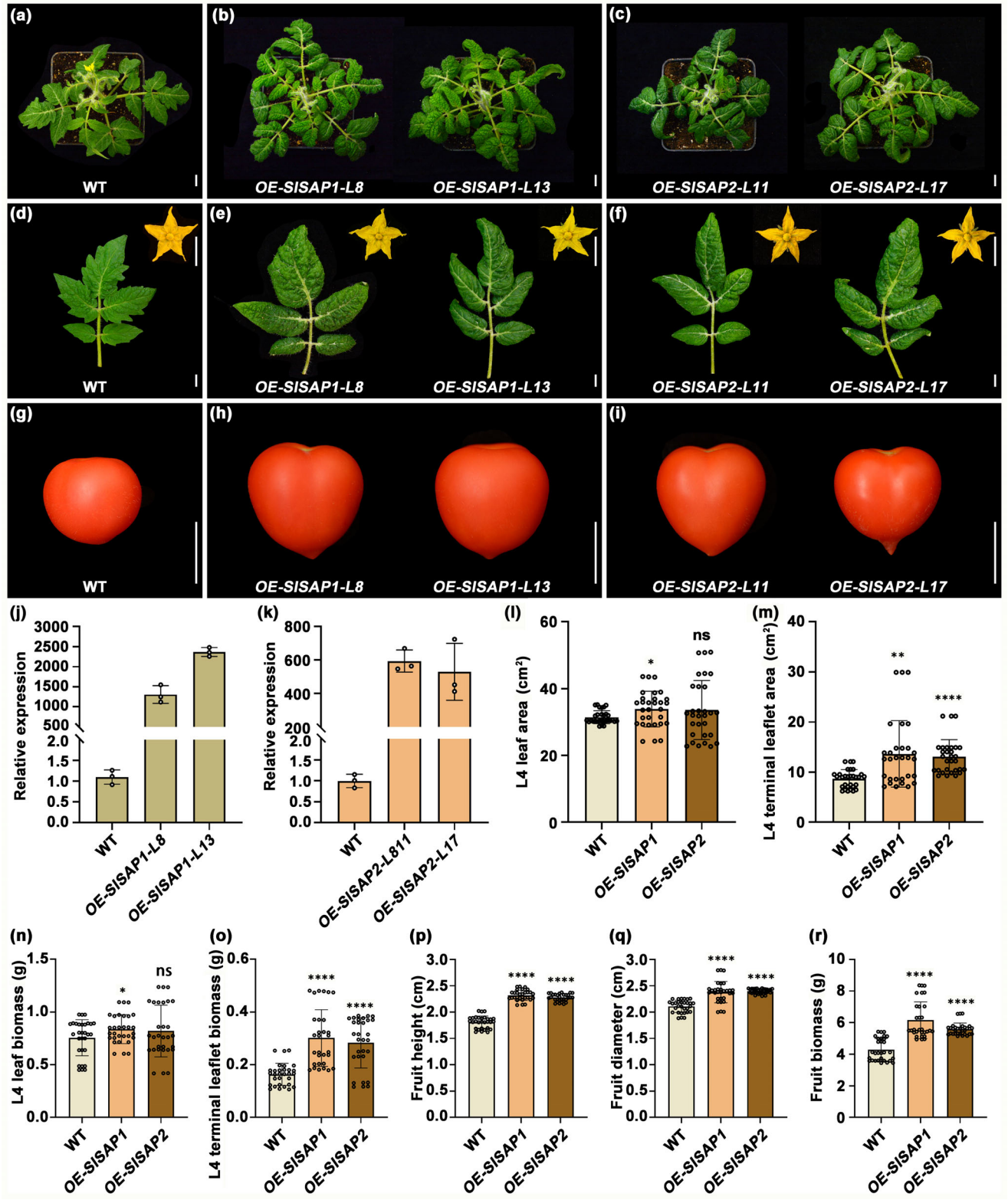

Fig. 4 Phenotypic characterization of the *STERILE APETALA1* (SlSAP1) and *STERILE APETALA12* (SlSAP2) overexpressing (OE) transgenic lines in tomato plants. (a–c) The plants of the indicated genotypes were grown in soil for 1 month under glasshouse conditions, as described in the Materials and Methods section, and photographed from the top. (d–f) Mature 5th leaves (count from the bottom) and the fully opened flowers (at the top right corner of each picture) of the indicated genotypes. (g–i) Red-ripening fruits of the indicated genotypes. (j) Quantitative real-time reverse-transcriptase PCR (qRT–PCR) analysis of the relative expression level of *SlSAP1* in *35S:SlSAP1-eGFP* transgenic lines (*OE-SlSAP1-L8* and *OE-SlSAP1-L13*). Error bars represent the SD of three biological replicates. (k) qRT–PCR analysis of the expression level of *SlSAP2* in *35S:SlSAP2-eGFP* transgenic lines (*OE-SlSAP2-L11* and *OE-SlSAP2-L17*). Error bars represent the SD of three biological replicates. *SlACTIN2* was used as the internal control in (j, k). (l–m) Quantification of the area of the 4th leaves (count from the bottom) (l) and its terminal leaflet (m) in the indicated genotypes. Error bars denote SE ($n = 30$). (n, o) Quantification of the biomass of the 4th leaves (count from the bottom) (n) and its terminal leaflet (o) in the indicated genotypes. Error bars denote SE ($n = 30$). (p–r) Quantification of the height (p), diameter (q), and biomass (r) of red-ripening fruits in the indicated genotypes. Error bars denote SE ($n = 30$). *t*-test: ns, not significant; *, $P < 0.05$; **, $P < 0.01$; ****, $P < 0.0001$. Bars: (a–i) 1 cm.

SlSAP2-overexpressed transgenic plants. These proteins were then mixed with equal amounts of *E. coli*-expressed MBP-SlKIX8 or MBP-SlKIX9 fusion proteins, followed by incubation at 4°C with gentle shaking. Samples were collected at different time points for gel quantification analysis. After 45 min of incubation, the amounts of MBP-SlKIX8 and MBP-SlKIX9 decreased compared to the initial levels in both the WT and the SlSAP1-overexpressed and SlSAP2-overexpressed plants (Fig. 7f,g). However, the degradation of MBP-SlKIX8 and MBP-SlKIX9 proteins was slower when incubated with the proteasome inhibitor MG132 (Fig. 7f,g), indicating that the stability of SlKIX8 and SlKIX9 is regulated by the proteasome. Furthermore, the degradation of MBP-SlKIX8 and MBP-SlKIX9 fusion proteins was significantly slower in samples incubated with total proteins from the *cr-slsap1 cr-slsap2* mutants but faster in samples incubated with proteins from the *SlSAP1*-overexpressed and *SlSAP2*-overexpressed lines compared to the WT (Fig. 7f,g). In addition, the further protein degradation experiment indicates the degradation of MBP-SlKIX8 and MBP-SlKIX9 fusion proteins was slightly faster in samples incubated with total proteins from *cr-slsap2* mutants than in those from *cr-slsap1* mutants (Fig. S8). These results suggest that the stability of SlKIX8 and SlKIX9 proteins is negatively regulated by SlSAP1 and SlSAP2 *in vitro*.

Taken together, these results suggest that SlSAP1 and SlSAP2 can form an SCF E3 ubiquitin ligase complex with SlASK1, SlASK2, and SlASK3 to modulate the stability of SlKIX8 and SlKIX9, thereby controlling leaf size and fruit size in tomato (Fig. 7h).

Discussion

As the economy has developed, tomato varieties have been bred to exhibit diverse colors, shapes, sizes, and flavor profiles, catering to consumers' evolving preferences for enjoyable and healthy eating (Kwon *et al.*, 2020; Cao *et al.*, 2024). Throughout the history of tomato domestication, fruit size has been a core trait. The wild tomato, *Solanum pimpinellifolium*, produces fruit weighing *c.* 1 g, while the domesticated variety, *S. lycopersicum* var. *lycopersicum*, can bear fruit exceeding 1 kg (Rodríguez *et al.*, 2011). The increase in fruit size has significantly improved yield and meets consumer demand for substantial production. In this study, we investigate the molecular mechanisms that determine tomato fruit size by identifying and characterizing two homologous *SAP* genes in tomato (Fig. 1a). Both the *cr-slsap1* and *cr-slsap2* mutant lines produce smaller fruits than the WT, and the fruits of the *cr-slsap1 cr-slsap2* double mutants show a more reduction in size (Figs 3k–n, S3l–n, S4j–p, S9a–d). Conversely, overexpression of either *SlSAP1* or *SlSAP2* results in enlarged fruits (Figs 4g–i, S9a–d). The variation in fruit size observed in the single and double mutants, as well as in the overexpressed transgenic lines, implies that modulating the abundance of the SAP proteins has the potential to produce fruits of various sizes.

Similar to other plant organs, the growth of fruit in tomato involves coordinated cell division and cell expansion. Previous reports have shown that *SAP* and its homologs play a conserved role in regulating fruit size in *M. truncatula*, Arabidopsis, and cucumber, as evidenced by the loss-of-function mutants (Wang *et al.*, 2016; Yang *et al.*, 2018; Yin *et al.*, 2020; Zhou *et al.*, 2021). Our study similarly indicates that tomato *SlSAP1* and *SlSAP2* are crucial regulators of fruit size (Figs 3k–n, 4g–i). However, it is worth noting that both Medicago and Arabidopsis produce dry fruits (legumes and siliques, respectively), and the processes of their development differ significantly from that of fleshy fruits like tomato. The underlying mechanism through which SAP regulates fleshy fruit size is still not fully understood. As a typical fleshy fruit, the fruit of tomato consists of the pericarp, locular tissue, columella, placenta, septum, and seeds (Mauxion *et al.*, 2021). In our study, we found that *SlSAP1* and *SlSAP2* redundantly regulate cell proliferation in the early stages of fruit development, leading to increased cell layers in the pericarp (Figs 5g–l,o, S10a–d). Additionally, the cell size is reduced in the loss-of-function lines and increased in the *SlSAP1* and *SlSAP2* overexpression lines, indicating that these genes positively regulate cell expansion during fruit development (Figs 5g–l,p, S10a–d). Therefore, *SlSAP1* and *SlSAP2* control tomato fruit size by promoting both cell proliferation and cell expansion in the pericarp. This is similar to other important fruit developmental regulators, such as *fruit weight 2.2* (*fw2.2*), *fw3.2*, *ASYMMETRIC LEAVES 2* (*SlAS2*), and *ASYMMETRIC LEAVES 2-LIKE* (*SlAS2L*) (Frary *et al.*, 2000; Nesbitt & Tanksley, 2001; Cong & Tanksley, 2006; Chakrabarti *et al.*, 2013; Dong *et al.*, 2023). Studies in *Medicago* and *Populus* have indicated that *SAP* homologs positively regulate cell number but negatively regulate cell size in leaves because of a compensation effect (Yordanov *et al.*, 2017; Zhou *et al.*, 2021). These effects differ from those observed in the leaf when *SlSAP1* and *SlSAP2* were knocked out (Fig. S11a–f), as cell number increases and cell size decreases in the leaf upon *SlSAP1* and *SlSAP2* knockout. This discrepancy suggests that the regulatory roles of SAPs in cell

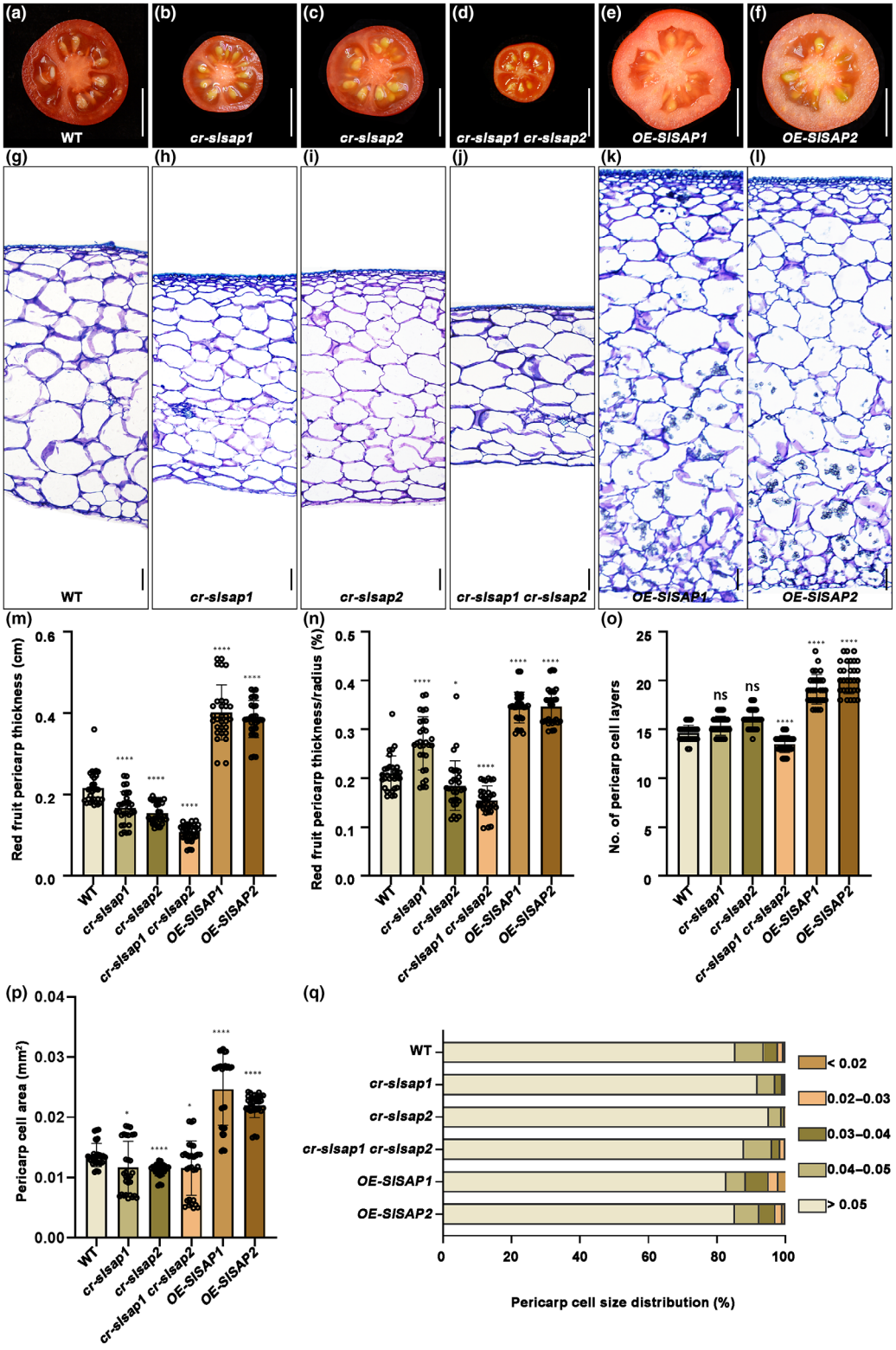

Fig. 5 Tomato cr-*slsap1 cr-slsap2* double mutants produce smaller fruits by reducing pericarp thickness. (a–f) Equatorial sections of red ripe fruits produced by wild-type (a), *cr-slsap1* (b), *cr-slsap2* (c), *cr-slsap1 cr-slsap2* (d), *35S:SlSAP1-eGFP* (OE-SlSAP1) (e), and *35S:SlSAP2-eGFP* (OE-SlSAP2) (f) genotypes. (g–l) Cross sections of the pericarp in 30 DPA fruits from wild-type (g), *cr-slsap1* (h), *cr-slsap2* (i), *cr-slsap1 cr-slsap2* (j), *35S:SlSAP1-eGFP* (OE-SlSAP1) (k), and *35S:SlSAP2-eGFP* (OE-SlSAP2) (l) lines. (m–n) Quantification of the pericarp thickness (m) and the percentage of the thickness relative to the radius (n) was performed in the indicated genotypes. (o) Number of pericarp cell layers in the indicated genotypes' fruits. (p) Pericarp cell area in the indicated genotypes' fruits. (q) Pericarp cell size distribution in the indicated genotypes fruits. Error bars denote SE ($n = 30$). DPA, days post-anthesis; SlSAP1, STERILE APETALA1. SlSAP2, STERILE APETALA2; OE, overexpression. GFP, green fluorescent protein. *t*-test: ns, not significant; *, $P < 0.05$; ****, $P < 0.0001$. Bars: (a–f) 1 cm; (g–l) 100 μm.

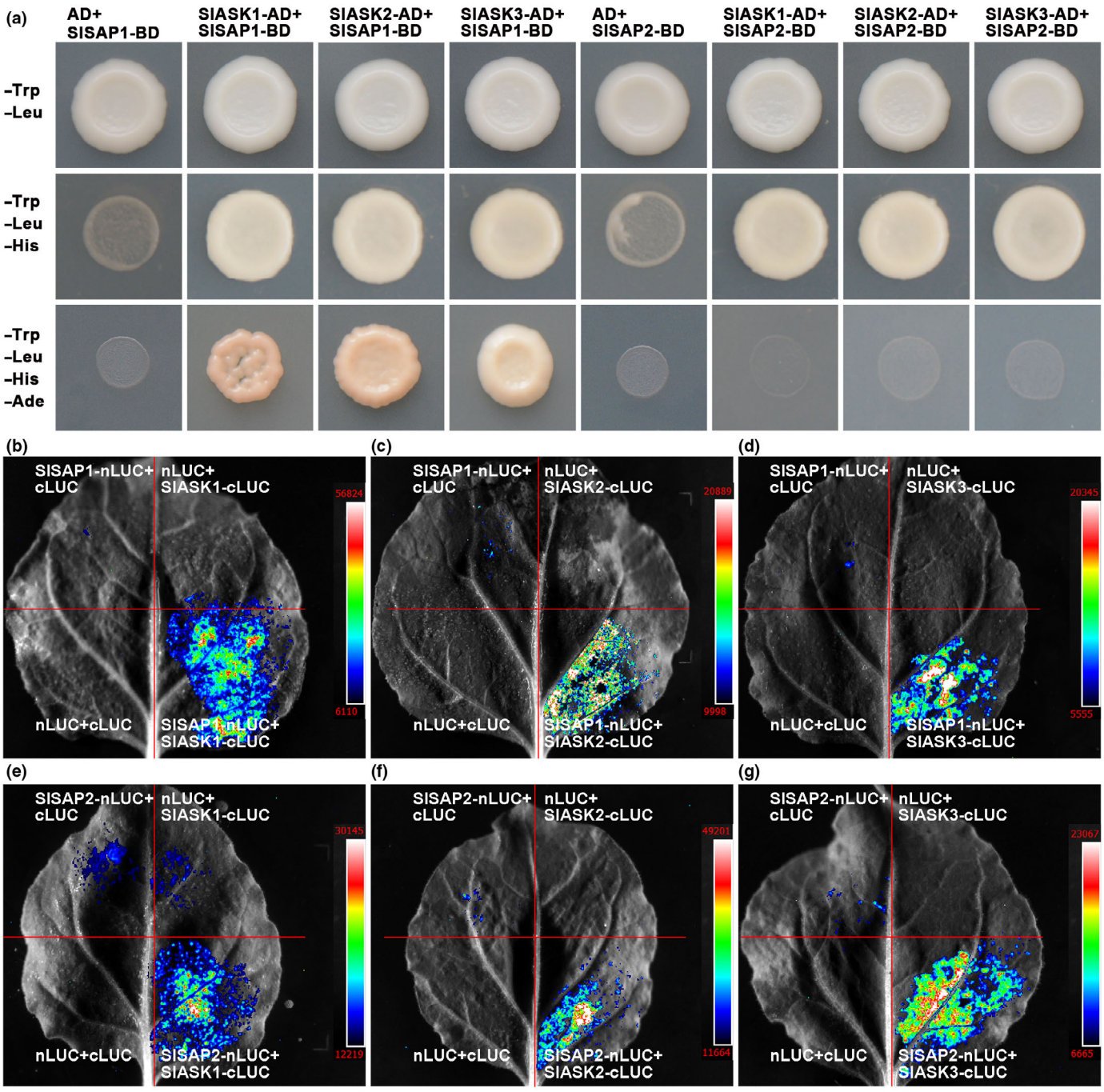

Fig. 6 The *STERILE APETALA1* (SlSAP1) and *STERILE APETALA2* (SlSAP2) proteins are components of the SKP1/Cullin1/F-box (SCF) complex to regulate organ size. (a) Interaction between SlSAP1 and SlSAP2 with SlASK1, SlASK2, and SlASK3 in a yeast two-hybrid (Y2H) assay. Auxotrophic growth indicates the interaction between different proteins. (b–g) Split luciferase (LUC) complementation assays demonstrated the interactions between SlSAP1/2 and SlASK1/2/3, where SlSAP1/2-nLUC and cLUC-SlASK1/2/3 were co-expressed in *Nicotiana benthamiana* leaves. Luciferase activity was detected 2 d later after infiltration.

proliferation and expansion during leaf development are species-specific, but the compensation effect appears to be a common response when cell division is disrupted. Nevertheless, in tomato fruits, mutations in *SlSAP1* and *SlSAP2* lead to reduced cell number and cell size in the pericarp (Fig. 5g–j,o–q), a phenomenon similar to the changes observed in cucumber leaves and petals upon knockout of *LL* in cucumber (Yang *et al.*, 2018). These results suggest that *SlSAP1*, *SlSAP2*, and their homologs play distinct cytological roles in regulating different lateral organs across different species.

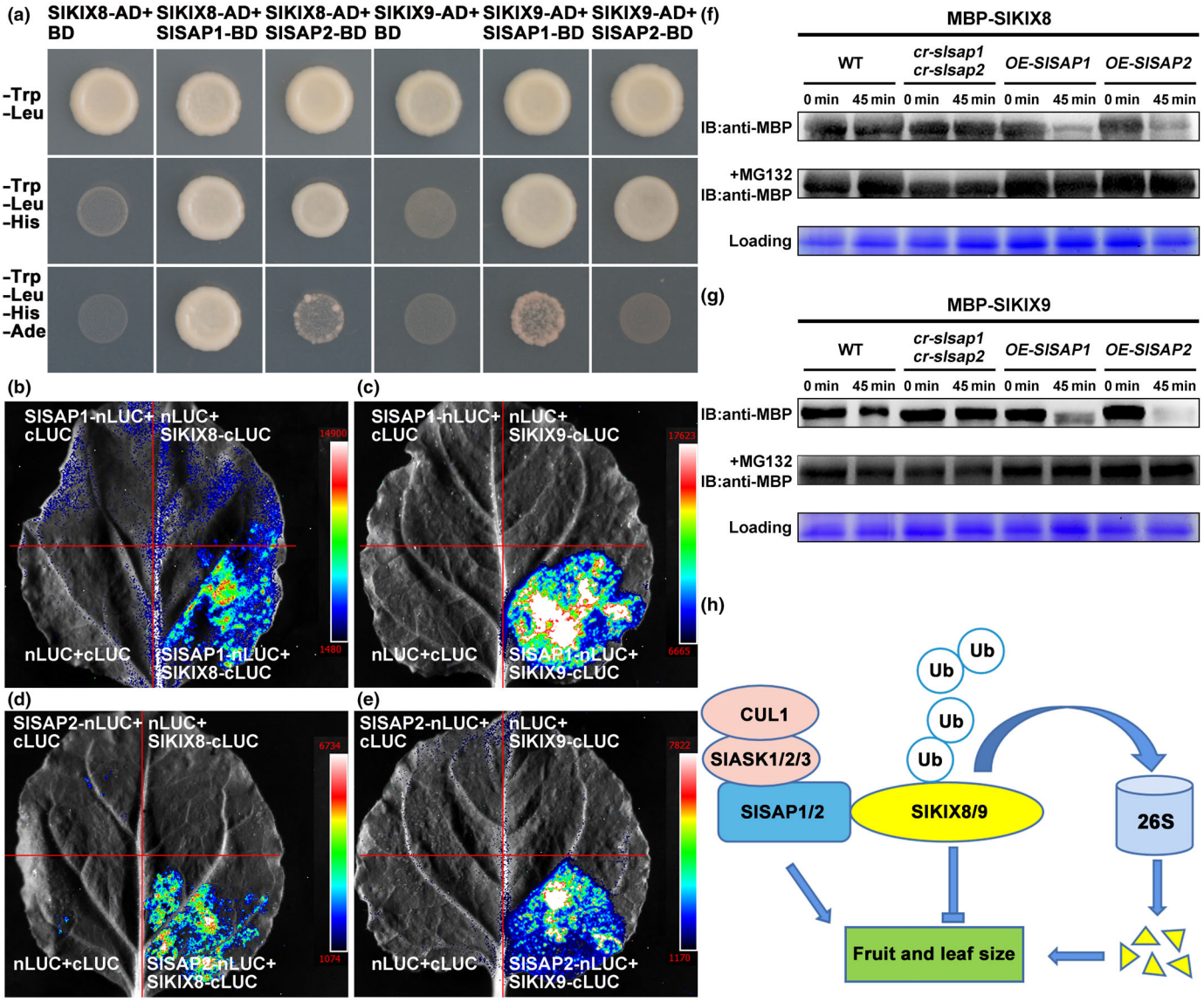

Fig. 7 *STERILE APETALA1* (SlSAP1) and *STERILE APETALA2* (SlSAP2) interact with and target SlKIX8 and SlKIX9 for degradation. (a) Interaction between SlSAP1 and SlSAP2 with SlKIX8 and SlKIX9 in a yeast two-hybrid (Y2H) assay. Auxotrophic growth indicates the interaction between different proteins. (b–e) The split luciferase complementation assay demonstrated the interactions between SlSAP1/2 and SlKIX8/9, where SlSAP1/2-nLUC and cLUC-SlKIX8/9 were coexpressed in *Nicotiana benthamiana* leaves. Luciferase activity was detected 2 d after infiltration. (f, g) SlSAP1 and SlSAP2 regulate SlKIX8 (f) and SlKIX9 (g) stability *in vitro*. The MBP-SlKIX8 and MBP-SlKIX9 fusion proteins were detected with the MBP antibody. MG132 was used to inhibit proteasome activity. Coomassie brilliant blue staining of the ACTIN2 protein was used as a loading control. (h) A model of SlSAP1 and SlSAP2 controlling fruit and leaf size. The $SCF^{SlSAP1/2}$ complex-mediated degradation of SlKIX8/9 proteins leads to increased fruit and leaf size.

Previous reports have indicated that the loss of function of *SAP* and its homologs in different species leads to a reduction in organ size. Conversely, overexpression of these homologous genes results in increased organ size (Schneider *et al.*, 2021). Similarly, our study demonstrates that *SlSAP1* and *SlSAP2* play redundant roles in controlling the size of leaves, flowers, and fruits in tomato (Figs 3g–n, 4d–i), suggesting that they share conserved functions with other eudicot species in regulating organ size. Notably, the *cr-slsap1 cr-slsap2* double mutants produce fewer leaflets than the WT (Fig. 3g,j), a phenotype that was not previously reported in other species. This suggests that *SlSAP1* and *SlSAP2* have a specific and distinct function on leaflet number in tomato, although the detailed mechanism remains unclear. The loss-of-function mutant of *SAP* in *Medicago* also exhibits species-specific phenotypic defects, such as specific defects in pulvinus development and leaf movement (Zhou *et al.*, 2021). These findings highlight that *SAP* homologs are crucial for certain species-specific biological functions across different species, potentially due to the involvement of ubiquitin-mediated protein degradation in various aspects of plant growth and development.

SAP is an F-box protein that functions as a component of the SCF complex, mediating the degradation of substrates such as

PPD1, PPD2, KIX8, and KIX9 in the ubiquitination pathway (Gonzalez *et al.*, 2015; Wang *et al.*, 2016; Li *et al.*, 2018; Liu *et al.*, 2020; Schneider *et al.*, 2021). Amino acid sequence alignment has shown that SlSAP1 and SlSAP2 share the conserved F-box motif in the N-terminal; both of them interact with the SKIP-like protein, SlASK1, SlASK2, and SlASK3 (Fig. 6a–g). In addition, the WD40 domain in the C-terminal regions of SlSAP1 and SlSAP2 mediates interaction with SlKIX8 and SlKIX9 (Fig. 7a–e), which are known as adaptors between PPD and TPL (Swinnen *et al.*, 2022; Mao *et al.*, 2023). Loss of function of *SlKIX8* and *SlKIX9* resulted in larger and dome-shaped leaves, as well as larger fruits in tomato (Swinnen *et al.*, 2022), similar to the transgenic lines that overexpress either *SlSAP1* or *SlSAP2* (Fig. 4d–i). Previous reports in Arabidopsis indicated KIX8 and KIX9 as novel substrates of SAP and negatively regulate meristemoid cell proliferation and final organ size (Li *et al.*, 2018). This raises the question of whether the SAP-KIX module has a function for tomato fruit size determination, and if so, how it works. Compared to other organs, such as flowers and leaves (Fig. 2a), the expression levels of *SlSAP1* and *SlSAP2* in red-ripe fruits are almost absent. However, *SlSAP1* and *SlSAP2* are slightly more highly expressed in 10–30 DPA fruits (Fig. S2), a key stage of cell expansion, even though their expression levels are low in tomato fruit overall. Some essential genes do not need a very high level of transcripts. For example, *PALMATE-LIKE PENTAFOLIATA1* (*PALM1*) has a very low level of expression in compound leaf tissue during the leaflet initiation stages, while loss-of-function *palm1* mutant has a severe leaf phenotype affecting leaflet number (Chen *et al.*, 2010). The ortholog of *SAP* in cucumber, *LL*, also regulates fruit size, decreasing fruit size in loss-of-function mutants and increasing fruit size in overexpression lines. This suggests that *SAP* regulation of fruit size is conserved, even though the expression level of *LL* is low in fruits (Yang *et al.*, 2018). The expression levels of both *SlKIX8* and *SlKIX9* are slightly higher in the immature green stage (Swinnen *et al.*, 2022), which overlaps with the expression of *SlSAP1* and *SlSAP2*. In addition, the almost indistinguishable phenotypes between transgenic lines overexpressing either *SlSAP1* or *SlSAP2* and the loss-of-function *SlKIX8* and *SlKIX9* mutants indicate that the SAP-KIX module regulates organ development in a global rather than in a localized way. Our results also indicate that both SlSAP1 and SlSAP2 interact with SlKIX8 and SlKIX9, and target them for degradation (Fig. 7a–g). These results suggest that the SAP-KIX module is also involved in organ size regulation in tomato.

Unlike a single functional *SAP* gene reported in many species, we identified two homologous *SAP* genes (*SlSAP1* and *SlSAP2*) from the tomato genome (Fig. 1a), which redundantly regulate fruit size. Interestingly, we found that these two *SAP* homologs are universally present in the Solanaceae family, including potato (*Solanum tuberosum*), pepper (*Capsicum annuum*), tobacco (*N. benthamiana*), and petunia (*Petunia hybrida*) (Fig. 1a). This may be related to the Solanum lineage experiencing two consecutive genome triplications (Consortium, 2012; J. Huang *et al.*, 2023). There are two *SAP* homologs in most diploid Solanaceae species, whereas most diploid legume species have only one *SAP* homolog, similar to Arabidopsis (Fig. 1a,b). This suggests that one of the *SAP* genes may have been lost in most diploid legume species and in Arabidopsis, or that *SlSAP2* was acquired through genome triplications. Paralogues arising from duplications can be functionally redundant, contributing to robust plant growth (Kwon *et al.*, 2022). It has been reported that a recessive mutation in the Arabidopsis *SAP* gene causes severe abnormalities in inflorescence, flower, and ovule development, ultimately leading to infertility (Byzova *et al.*, 1999). A similar phenotype was also observed in the *Medicago SMALL LEAF AND BUSHY1* (*SLB1*)/*MINI ORGAN1* (*MIO1*) mutants (Yin *et al.*, 2020; Zhou *et al.*, 2021). In our study, the single mutant *cr-slsap1* exhibited no morphological abnormalities in the four types of floral organs, and flower fertility is equal to that of the WT, except for the narrower petals (Fig. 3g,h). This is due to the presence of another *SAP* homolog in the tomato genome. Consistently, the *cr-slsap1 cr-slsap2* double mutants exhibit more severe dwarfism, smaller fruit size, and apparent defects in fertility (Fig. 3c,g,k,f,j,n). Notably, in the cucumber inbred line H19, a T to G base substitution in the *LL* gene resulted in an amino acid change from tryptophan to glycine at the 264th position (W264G). The *LITTLELEAF* (*LL*) mutants are able to produce smaller fruit despite having only one *SAP* homolog in cucumber (Yang *et al.*, 2018). It appears that the *LL* mutants are weak allelic mutants, as they involve only a single amino acid change in the LL amino acid sequence. Thus, the presence of double *SAP* homologs in the tomato genome, as well as in other Solanaceae species, ensures proper fruit growth and development.

Acknowledgements

The authors thank Dr Junqing Wu for the valuable suggestions for this research. This work was supported by the National Natural Science Foundation of China (32200681, 32170360, 32470334, and U2102222), Strategic Priority Research Programs of the Chinese Academy of Sciences (Grant no. XDA26030301), Youth Innovation Promotion Association CAS (2021395), and Yunnan Revitalization Talent Support Program (Grant nos. XDYC-QNRC-79, XDYC-QNRC-2022-0179, and XDYC-QNRC-2022-0335).

Competing interests

None declared.

Author contributions

JC, LY, LH and SW conceived and designed the experiments. WL, ML and LY performed most of the experiments. RW, BZ, YM, DW, QW, SZ, JY, XJ, XX and YL helped with the experiments. LY and WL wrote the manuscript. JC, LY, LH, SZ and QW revised the manuscript. All the authors have read and approved the paper. WL and ML contributed equally to this work.

ORCID

Jianghua Chen https://orcid.org/0000-0003-0715-1859
Liangliang He https://orcid.org/0000-0002-2169-4326
Shuang Wu https://orcid.org/0000-0003-1913-8125
Baolin Zhao https://orcid.org/0000-0001-8082-4461

Data availability

Gene sequence data of this article can be found in the *Solanum lycopersicum* ITAG v.5.0 of the PHYTOZOME database (https://phytozome-next.jgi.doe.gov/), SlSAP1 is annotated as Solyc05G001777 and SlSAP2 as Solyc07G001756. Sequence data of this article can also be found in the PHYTOZOME database (https://phytozome-next.jgi.doe.gov/) under the following accession nos.: SlSAP1 (Solyc05g041220); SlSAP2 (Solyc07g045550); SlASK1 (Solyc11g042930); SlASK2 (Solyc01g111650); SlASK3 (Solyc10g055580); SlKIX8 (Solyc07g008100); SlKIX9 (Solyc08g059700); SlACTIN2 (Solyc11g005330) in the old version. It is worth noting that the annotated amino acid sequence of SlSAP2 (Solyc07g045550) in the PHYTOZOME database is partial and does not represent the full-length CDS.

References

Aguirre L, Hendelman A, Hutton SF, Mccandlish DM, Lippman ZB. 2023. Idiosyncratic and dose-dependent epistasis drives variation in tomato fruit size. *Science* **382**: 315–320.

Azeez A, Busov V. 2021. CRISPR/Cas9-mediated single and biallelic knockout of poplar *STERILE APETALA* (*PopSAP*) leads to complete reproductive sterility. *Plant Biotechnology Journal* **19**: 23–25.

Azzi L, Deluche C, Gévaudant F, Frangne N, Delmas F, Hernould M, Chevalier C. 2015. Fruit growth-related genes in tomato. *Journal of Experimental Botany* **66**: 1075–1086.

Byzova MV, Franken J, Aarts MG, de Almeida-Engler J, Engler G, Mariani C, Van Lookeren CM, Angenent GC. 1999. Arabidopsis *STERILE APETALA*, a multifunctional gene regulating inflorescence, flower, and ovule development. *Genes & Development* **13**: 1002–1014.

Cao Y, She J, Li Z, Liu Y, Tian T, You Q, Yan H, Ma X, Xu W, Su Z. 2024. TomAP: a multi-omics data analysis platform for advancing functional genomics research in tomatoes. *New Crops* **1**: 100002.

Chakrabarti M, Zhang N, Sauvage C, Muños S, Blanca J, Cañizares J, Diez MJ, Schneider R, Mazourek M, Mcclead J *et al.* 2013. A cytochrome P450 regulates a domestication trait in cultivated tomato. *Proceedings of the National Academy of Sciences, USA* **110**: 17125–17130.

Chen J, Yu J, Ge L, Wang H, Berbel A, Liu Y, Chen Y, Li G, Tadege M, Wen J *et al.* 2010. Control of dissected leaf morphology by a Cys(2)His(2) zinc finger transcription factor in the model legume *Medicago truncatula*. *Proceedings of the National Academy of Sciences, USA* **107**: 10754–10759.

Chu YH, Jang JC, Huang Z, Knaap E. 2019. Tomato locule number and fruit size controlled by natural alleles of *lc* and *fas*. *Plant Direct* **3**: e00142.

Cong B, Tanksley SD. 2006. FW2.2 and cell cycle control in developing tomato fruit: a possible example of gene co-option in the evolution of a novel organ. *Plant Molecular Biology* **62**: 867–880.

Dong R, Yuan Y, Liu Z, Sun S, Wang H, Ren H, Cui X, Li R. 2023. *ASYMMETRIC LEAVES 2* and *ASYMMETRIC LEAVES 2-LIKE* are partially redundant genes and essential for fruit development in tomato. *The Plant Journal* **114**: 1285–1300.

Frary A, Nesbitt TC, Grandillo S, Knaap E, Cong B, Liu J, Meller J, Elber R, Alpert KB, Tanksley SD. 2000. *fw2.2:* a quantitative trait locus key to the evolution of tomato fruit size. *Science* **289**: 85–88.

Gonzalez N, Pauwels L, Baekelandt A, De Milde L, Van Leene J, Besbrugge N, Heyndrickx KS, Pérez AC, Durand AN, De Clercq R *et al.* 2015. A repressor protein complex regulates leaf growth in Arabidopsis. *Plant Cell* **27**: 2273–2287.

Huang H, Qiao H, Ma X, Zhao W, Sun L, Yang R, Wang S. 2023. Roles of jasmonates in tomato growth, development and defense. *Vegetable Research* **3**: 14.

Huang J, Xu W, Zhai J, Hu Y, Guo J, Zhang C, Zhao Y, Zhang L, Martine C, Ma H *et al.* 2023. Nuclear phylogeny and insights into whole-genome duplications and reproductive development of Solanaceae plants. *Plant Communications* **4**: 100595.

Huang S, Liu W, Xu J, Liu Z, Li C, Feng H. 2020. The *SAP* function in pistil development was proved by two allelic mutations in Chinese cabbage (*Brassica rapa* L. ssp. *pekinensis*). *BMC Plant Biology* **20**: 538.

Kwon C, Heo J, Lemmon ZH, Capua Y, Hutton SF, Van Eck J, Park SJ, Lippman ZB. 2020. Rapid customization of Solanaceae fruit crops for urban agriculture. *Nature Biotechnology* **38**: 182–188.

Kwon CT, Tang L, Wang X, Gentile I, Hendelman A, Robitaille G, Van Eck J, Xu C, Lippman ZB. 2022. Dynamic evolution of small signalling peptide compensation in plant stem cell control. *Nature Plants* **8**: 346–355.

Li N, Liu Z, Wang Z, Ru L, Gonzalez N, Baekelandt A, Pauwels L, Goossens A, Xu R, Zhu Z *et al.* 2018. STERILE APETALA modulates the stability of a repressor protein complex to control organ size in *Arabidopsis thaliana*. *PLoS Genetics* **14**: e1007218.

Li N, Xu R, Li Y. 2019. Molecular networks of seed size control in plants. *Annual Review of Plant Biology* **70**: 435–463.

Liu L, Zhang Y, Tang S, Zhao Q, Zhang Z, Zhang H, Dong L, Guo H, Xie Q. 2010. An efficient system to detect protein ubiquitination by agroinfiltration in *Nicotiana benthamiana*. *The Plant Journal* **61**: 893–903.

Liu W, Huang S, Liu Z, Lou T, Tan C, Wang Y, Feng H. 2019. A missense mutation of *STERILE APETALA* leads to female sterility in Chinese cabbage (*Brassica campestris* ssp. *pekinensis*). *Plant Reproduction* **32**: 217–228.

Liu X, Hou J, Chen L, Li Q, Fang X, Wang J, Hao Y, Yang P, Wang W, Zhang D *et al.* 2022. Natural variation of *GhSI7* increases seed index in cotton. *Theoretical and Applied Genetics* **135**: 3661–3672.

Liu Y, Yang Y, Wang R, Liu M, Ji X, He Y, Zhao B, Li W, Mo X, Zhang X *et al.* 2023. Control of compound leaf patterning by *MULTI-PINNATE LEAF1* (*MPL1*) in chickpea. *Nature Communications* **14**: 8088.

Liu Z, Li N, Zhang Y, Li Y. 2020. Transcriptional repression of *GIF1* by the KIX-PPD-MYC repressor complex controls seed size in *Arabidopsis*. *Nature Communications* **11**: 1846.

Mao Y, Zhou S, Yang J, Wen J, Wang D, Zhou X, Wu X, He L, Liu M, Wu H *et al.* 2023. The MIO1-MtKIX8 module regulates the organ size in *Medicago truncatula*. *Physiologia Plantarum* **175**: e14046.

Mauxion JP, Chevalier C, Gonzalez N. 2021. Complex cellular and molecular events determining fruit size. *Trends in Plant Science* **26**: 1023–1038.

Monforte AJ, Diaz A, Caño-Delgado A, van der Knaap E. 2014. The genetic basis of fruit morphology in horticultural crops: lessons from tomato and melon. *Journal of Experimental Botany* **65**: 4625–4637.

Mu Q, Huang Z, Chakrabarti M, Illa-Berenguer E, Liu X, Wang Y, Ramos A, van der Knaap E. 2017. Fruit weight is controlled by cell size regulator encoding a novel protein that is expressed in maturing tomato fruits. *PLoS Genetics* **13**: e1006930.

Nesbitt TC, Tanksley SD. 2001. *fw2.2* directly affects the size of developing tomato fruit, with secondary effects on fruit number and photosynthate distribution. *Plant Physiology* **127**: 575–583.

Rieu P, Arnoux-Courseaux M, Tichtinsky G, Parcy F. 2023. Thinking outside the F-box: how UFO controls angiosperm development. *New Phytologist* **240**: 945–959.

Rodríguez GR, Muños S, Anderson C, Sim S, Michel A, Causse M, Gardener BBM, Francis D, van der Knaap E. 2011. Distribution of SUN, OVATE, LC, and FAS in the tomato germplasm and the relationship to fruit shape diversity. *Plant Physiology* **156**: 275–285.

Saxena H, Negi H, Sharma B. 2023. Role of F-box E3-ubiquitin ligases in plant development and stress responses. *Plant Cell Reports* **42**: 1133–1146.

Schneider M, Gonzalez N, Pauwels L, Inzé D, Baekelandt A. 2021. The PEAPOD pathway and its potential to improve crop yield. *Trends in Plant Science* **26**: 220–236.

Sicard A, Kappel C, Lee YW, Woźniak NJ, Marona C, Stinchcombe JR, Wright SI, Lenhard M. 2016. Standing genetic variation in a tissue-specific enhancer underlies selfing-syndrome evolution in *Capsella*. *Proceedings of the National Academy of Sciences, USA* **113**: 13911–13916.

Swinnen G, Mauxion J, Baekelandt A, De Clercq R, Van Doorsselaere J, Inzé D, Gonzalez N, Goossens A, Pauwels L. 2022. SlKIX8 and SlKIX9 are negative regulators of leaf and fruit growth in tomato. *Plant Physiology* **188**: 382–396.

Tanksley SD. 2004. The genetic, developmental, and molecular bases of fruit size and shape variation in tomato. *Plant Cell* **16**: S181–S189.

Tomato Genome Consortium. 2012. The tomato genome sequence provides insights into fleshy fruit evolution. *Nature* **485**: 635–641.

Tran TM, Billakurthi K. 2024. Tomato FW2.2/CNR might regulate fruit size via plasmodesmata callose deposition. *Plant Physiology* **196**: 679–680.

Varshney V, Majee M. 2022. Emerging roles of the ubiquitin-proteasome pathway in enhancing crop yield by optimizing seed agronomic traits. *Plant Cell Reports* **41**: 1805–1826.

Wang P, Li Z, Li H, Zhang D, Wang W, Xu X, Xie Q, Duan Z, Xia X, Guo G *et al.* 2024. Smart crops. *New Crops* **1**: 100007.

Wang X, Feng S, Nakayama N, Crosby WL, Irish V, Deng XW, Wei N. 2003. The COP9 signalosome interacts with SCF^{UFO} and participates in Arabidopsis flower development. *Plant Cell* **15**: 1071–1082.

Wang Z, Li N, Jiang S, Gonzalez N, Huang X, Wang Y, Inzé D, Li Y. 2016. SCF^{SAP} controls organ size by targeting PPD proteins for degradation in *Arabidopsis thaliana*. *Nature Communications* **7**: 11192.

White DW. 2006. PEAPOD regulates lamina size and curvature in Arabidopsis. *Proceedings of the National Academy of Sciences, USA* **103**: 13238–13243.

Xu C, Liberatore KL, Macalister CA, Huang Z, Chu YH, Jiang K, Brooks C, Ogawa-Ohnishi M, Xiong G, Pauly M *et al.* 2015. A cascade of arabinosyltransferases controls shoot meristem size in tomato. *Nature Genetics* **47**: 784–792.

Yang L, Liu H, Zhao J, Pan Y, Cheng S, Lietzow CD, Wen C, Zhang X, Weng Y. 2018. LITTLELEAF (LL) encodes a WD40 repeat domain-containing protein associated with organ size variation in cucumber. *The Plant Journal* **95**: 834–847.

Yang L, Qi S, Touqeer A, Li H, Zhang X, Liu X, Wu S. 2020. *SlGT11* controls floral organ patterning and floral determinacy in tomato. *BMC Plant Biology* **20**: 562.

Yin J, Niu L, Li Y, Song X, Ottosen C-O, Wu Z, Jiang F, Zhou R. 2023. The effects of waterlogging stress on plant morphology, leaf physiology and fruit yield in six tomato genotypes at anthesis stage. *Vegetable Research* **3**: 31.

Yin P, Ma Q, Wang H, Feng D, Wang X, Pei Y, Wen J, Tadege M, Niu L, Lin H. 2020. SMALL LEAF AND BUSHY1 controls organ size and lateral branching by modulating the stability of BIG SEEDS1 in *Medicago truncatula*. *New Phytologist* **226**: 1399–1412.

Yordanov YS, Ma C, Yordanova E, Meilan R, Strauss SH, Busov VB. 2017. BIG LEAF is a regulator of organ size and adventitious root formation in poplar. *PLoS ONE* **12**: e180527.

Yuste-Lisbona FJ, Fernández-Lozano A, Pineda B, Bretones S, Ortíz-Atienza A, García-Sogo B, Müller NA, Angosto T, Capel J, Moreno V *et al.* 2020. *ENO* regulates tomato fruit size through the floral meristem development network. *Proceedings of the National Academy of Sciences, USA* **117**: 8187–8195.

Zhao X, Muhammad N, Zhao ZX, Yin KL, Liu ZG, Wang LX, Luo Z, Wang LH, Liu MJ. 2021. Molecular regulation of fruit size in horticultural plants: a review. *Scientia Horticulturae* **288**: 110353.

Zhou S, Yang T, Mao Y, Liu Y, Guo S, Wang R, Fangyue G, He L, Zhao B, Bai Q *et al.* 2021. The F-box protein MIO1/SLB1 regulates organ size and leaf movement in *Medicago truncatula*. *Journal of Experimental Botany* **72**: 2995–3011.

Zsögön A, Čermák T, Naves ER, Notini MM, Edel KH, Weinl S, Freschi L, Voytas DF, Kudla J, Peres LEP. 2018. *De novo* domestication of wild tomato using genome editing. *Nature Biotechnology* **36**: 1211–1216.

Supporting Information

Additional Supporting Information may be found online in the Supporting Information section at the end of the article.

Dataset S1 Data of a full maximum-likelihood tree of 33 species SAP sequences.

Fig. S1 Multiple sequence alignment of SlSAP1, SlSAP2, and their homologs.

Fig. S2 qRT-PCR analysis of the relative expression levels of *SlSAP1* and *SlSAP2* in different fruit development periods.

Fig. S3 *SlSAP1* and *SlSAP2* positively regulate organ size in tomato MT ecotype.

Fig. S4 *SlSAP1* and *SlSAP2* positively regulate organ size in tomato AC ecotype.

Fig. S5 Fruit size from tomato wild-type and *sl-sap1 sl-sap2* plants grown in restricted conditions is increased.

Fig. S6 Yeast two-hybrid cDNA library screening for factors interacting with SlSAP1.

Fig. S7 Yeast two-hybrid interaction analysis of SlSAP1 and SlSAP2 with SlPPD1 and SlPPD2 proteins.

Fig. S8 SlSAP1 and SlSAP2 regulate SlKIX8 and SlKIX9 stability *in vitro*.

Fig. S9 Comparison of fruit development from anthesis to ripening in tomato wild-type, *cr-slsap1*, *cr-slsap2*, *cr-slsap1 cr-slsap2*, *OE-SlSAP1*, and *OE-SlSAP2* transgenic lines.

Fig. S10 Comparison of cell layers and cell size during fruit development in tomato wild-type, *cr-slsap1*, *cr-slsap2*, *cr-slsap1 cr-slsap2*, *OE-SlSAP1*, and *OE-SlSAP2* transgenic lines.

Fig. S11 Variation in the size and number of pavement cells in the epidermis of mature leaves.

Table S1 Primer sequences used in this study.

Please note: Wiley is not responsible for the content or functionality of any Supporting Information supplied by the authors. Any queries (other than missing material) should be directed to the *New Phytologist* Central Office.